Quantitative Prediction of Human Intestinal Glucuronidation Effects on Intestinal Availability of UDP-Glucuronosyltransferase Substrates Using In Vitro Data[S]

Fumihiro Nakamori, Yoichi Naritomi, Ken-ichi Hosoya, Hiroyuki Moriguchi, Kazuhiro Tetsuka, Takako Furukawa, Keitaro Kadono, Katsuhiro Yamano, Shigeyuki Terashita, and Toshio Teramura

Analysis and Pharmacokinetics Research Laboratories, Discovery Drug Metabolism and Pharmacokinetics, Astellas Pharma, Inc., Ibaraki, Japan (F.N., Y.N., H.M., K.T., T.F., K.K., K.Y., S.T., T.T.); and Department of Pharmaceutics, Graduate School of Medicine and Pharmaceutical Sciences, University of Toyama, Toyama, Japan (F.N., K.H.)

ABSTRACT:

We investigated whether the effects of intestinal glucuronidation on the first-pass effect can be predicted from in vitro data for UDP-glucuronosyltransferase (UGT) substrates. Human in vitro intrinsic glucuronidation clearance ($CL_{int,\ UGT}$) for 11 UGT substrates was evaluated using pooled intestinal microsomes (4.00–4620 $\mu l \cdot min^{-1} \cdot mg^{-1}$) and corrected by the free fraction in the microsomal mixture ($CLu_{int,\ UGT}$ = 5.2–5133 $\mu l \cdot min^{-1} \cdot mg^{-1}$). Eleven UGT substrates were stable against intestinal cytochrome P450, indicating intestinal glucuronidation has a main effect on human intestinal availability. Oral absorbability intestinal availability (F_aF_g) values were calculated from in vivo pharmacokinetic parameters in the literature (F_aF_g = 0.01–1.0). It was found that $CLu_{int,\ UGT}$ and human F_aF_g have an inverse relationship that can be fitted to a simplified intestinal availability model. Experiments using Supersomes from insect cells expressing UGT isoforms showed that the substrates used were conjugated by various UGT isoforms. These results suggest that combining the simplified intestinal availability model and in vitro conjugation assay make it possible to predict human F_aF_g regardless of UGT isoform.

Introduction

Because many drugs are metabolized by UDP-glucuronosyltransferases (UGTs) (Williams et al., 2004), the related conjugation reaction glucuronidation may contribute to the pharmacokinetics of these drugs. Although hepatic glucuronidation has received more interest, attention to intestinal glucuronidation has been growing (Cubitt et al., 2009; Mizuma, 2009). A good example is raloxifene, which is used in the prevention of osteoporosis in postmenopausal woman. This drug is a substrate for UGT1A8 and UGT1A10, and glucuronidation is associated with low human bioavailability (Mizuma, 2009), which is expressed as the product of oral absorbability (F_a), intestinal availability (F_g), and hepatic availability (F_h). UGT1A8 and UGT1A10 are unlike most of the other 17 known UGT isoforms because they are expressed in the human intestine, not liver (Ohno and Nakajin, 2009). Despite evidence that intestinal glucuronidation may affect drug pharmacokinetics in humans, there are only limited tools for predicting the human F_aF_g of drugs metabolized by intestinal UGTs.

One method is the simplified intestinal availability (SIA) model (Kadono et al., 2010), which predicts human F_aF_g from in vitro data for highly permeable CYP3A4 substrates as shown in eq. 1:

$$F_aF_g = \frac{1}{1 + \alpha\, CL_{met,P450}} \quad (1)$$

where $CL_{met,\ P450}$ represents the in vitro intrinsic intestinal clearance ($CL_{int,\ P450}$) normalized by the $CL_{int,\ P450}$ of midazolam and α represents an empirical scaling factor, which is obtained from the relationship between F_aF_g and $CL_{met,\ P450}$ for drugs with human F_aF_g data. The SIA model can even be used to predict the F_aF_g of drugs that are highly permeable P-glycoprotein (P-gp) substrates. P-gp is an efflux transporter in human intestine and has the potential to reduce drug absorption. More importantly for this study, the SIA model has also been reported to predict the F_aF_g of UGT substrates in rats (Furukawa et al., 2012). However, its ability to predict human F_aF_g

ABBREVIATIONS: UGT, UDP-glucuronosyltransferase; F_a, oral absorbability; F_g, intestinal availability; F_h, hepatic availability; SIA, simplified intestinal availability; P-gp, P-glycoprotein; HIM, human intestinal microsomes; LC-MS/MS, liquid chromatography-tandem mass spectrometry; RED, rapid equilibrium dialysis; $f_{u,\ mic}$, unbound fraction of the microsomal mixture; R_b, blood/plasma ratio; $CL_{int,\ UGT}$, in vitro intrinsic glucuronidation clearance; $CLu_{int,\ UGT}$, unbound in vitro intrinsic glucuronidation clearance; PAMPA, parallel artificial membrane permeability assay; P450, cytochrome P450; COMT, catechol-O-methyltransferase enzyme; AUC, area under the concentration-time curve; GlcUA, glucuronic acid; hr, human recombinant.

values of UGT substrates remains unclear. Therefore, the aims of this study were to investigate the relationship between in vitro human intestinal glucuronidation clearance and F_aF_g in humans and to clarify whether intestinal availability of UGT substrates can be predicted using the SIA model.

Materials and Methods

Materials. Raloxifene, tolcapone, and entacapone were purchased from Toronto Research Chemicals Inc. (North York, ON, Canada). Quercetin, diclofenac, tolfenamic acid, gemfibrozil, indomethacin, and UDP-GlcUA were purchased from Sigma-Aldrich (St. Louis, MO). Telmisartan and etodolac were purchased from LKT Laboratories (St. Paul, MN). Bazedoxifene was purchased from Chemtos, LLC Laboratories (Austin, TX). Pooled human intestinal microsomes (HIM; $n = 10$) were purchased from XenoTech, LLC (Lenexa, KS). Recombinant UGT Supersomes (UGT1A1, UGT1A3, UGT1A4, UGT1A6–UGT1A10, UGT2B4, UGT2B7, UGT2B15, and UGT2B17) expressed in baculovirus-infected insect cells were purchased from BD Gentest (Woburn, MA). All other chemicals and reagents were of an analytical grade and readily available from commercial sources.

In Vitro Glucuronidation. In vitro glucuronidation was measured using a procedure published previously (Nakamori et al., 2011). Except for quercetin and telmisartan, each substrate was dissolved in 50% acetonitrile to 50 μM. Quercetin was dissolved to 500 μM because of the detection range limit. Telmisartan was dissolved in 50% acetonitrile with equal amounts of NaOH. These substrate solutions were incubated in a reaction mixture consisting of pooled HIM (final concentration, 0.02–0.4 mg/ml) in the presence of Tris-HCl buffer (50 mM, pH 7.4), magnesium chloride (8 mM), and alamethicin at a final concentration of 50 μg/mg microsomal protein. After preincubation at 37°C, UDP-GlcUA was added to initiate the enzyme reaction (final concentration, 2 mM). Each substrate solution was added to the reaction mixture until a final substrate concentration of 0.1 μM (the acetonitrile concentration in the reaction mixture was 0.1%) except for quercetin, which had a final concentration of 1.0 μM. The reaction was terminated at predetermined time points by mixing the reaction mixture with a 2-fold volume of chilled acetonitrile, followed by centrifugation at 15,000g for 5 min at 4°C. An aliquot of the supernatant was diluted twice with 0.1% formic acid and was injected into a liquid chromatography-tandem mass spectrometry (LC-MS/MS) apparatus to measure the concentration of unchanged compound. Intrinsic clearance values were calculated on the basis of the rate of substrate disappearance within the reaction mixture.

Cytochrome P450 Metabolism. Each substrate standard solution was prepared as described above for in vitro glucuronidation. These substrate solutions were incubated in a reaction mixture consisting of HIM (final concentration, 0.4 mg/ml) in the presence of potassium phosphate buffer (100 mM, pH 7.4) and EDTA (0.1 mM). Each substrate solution was added to the reaction mixture until a final substrate concentration of 0.1 μM (the acetonitrile concentration in the reaction mixture was 0.1%) except for quercetin, which had a final concentration of 1.0 μM. After preincubation at 37°C, NADPH was added to initiate the enzyme reaction. The reaction was terminated at 0, 30, 60, and 120 min by mixing the reaction mixture with a 2-fold volume of chilled acetonitrile, followed by centrifugation at 15,000g for 5 min at 4°C. An aliquot of the supernatant was diluted twice with 0.1% formic acid and was injected into an LC-MS/MS apparatus to measure the concentration of unchanged compound. Intrinsic clearance values were calculated on the basis of the rate of substrate disappearance within the reaction mixture.

Free Fraction in the Microsomal Mixture. The free fraction in the reaction mixture for all substrates except quercetin was determined at protein concentrations of 0.02, 0.2, and 0.4 mg/ml using a disposable 96-well rapid equilibrium dialysis (RED) plate (Thermo Fisher Scientific, Waltham, MA). The dialysis membrane had an 8-kDa molecular mass cutoff. Substrates were added to the acceptor side of the RED plate with the above reaction mixture minus UDP-GlcUA. Tris-HCl (50 mM), MgCl$_2$ (8 mM), and alamethicin (10 μg/ml) were added to the acceptor side of the RED plate. The RED plate was sealed, and dialysis was performed for 6 h at 37°C. After incubation, 30 μl of the acceptor side and 30 μl of the donor side were removed by siphoning, and the concentrations of the unchanged compounds were determined by LC-MS/MS. The unbound fraction of the microsomal mixture ($f_{u, mic}$) was calculated by eq. 2:

$$f_{u,mic} = \text{(unchanged compound concentration in acceptor side)}$$
$$/\text{(unchanged compound concentration in donor side)} \quad (2)$$

When correcting for the unbound fraction within the microsomal mixture, $CLu_{int, UGT}$ was defined as eq. 3:

$$CLu_{int,UGT} = CL_{int, UGT}/f_{u,mic} \quad (3)$$

However, quercetin was extensively adsorbed to the dialysis membrane, preventing the determination of its $f_{u, mic}$. Therefore, this value was cited from a previous study (Cubitt et al., 2009).

Human Recombinant UGT Reaction Screening. Human recombinant UGT reaction screening was performed with 12 commercially available human recombinant UGT Supersomes (hrUGTs). Each standard solution was incubated in a reaction mixture consisting of hrUGTs (final concentration, 0.2 mg/ml) and UDP-GlcUA (final concentration, 2 mM) in the presence of Tris-HCl buffer (50 mM, pH 7.4), magnesium chloride (8 mM), and alamethicin at a final concentration of 50 μg/mg microsomal protein. Each substrate solution was added to give a final substrate concentration of 0.1 μM (the acetonitrile concentration in the reaction mixture was 0.1%) except for quercetin, which had a final concentration of 1.0 μM. After preincubation at 37°C, UDP-GlcUA was added to initiate the enzyme reaction. The reaction was terminated at 30 min by mixing it with a 2-fold volume of chilled acetonitrile, followed by centrifugation at 15,000g for 5 min at 4°C. An aliquot of the supernatant was diluted twice with 0.1% formic acid and was injected into an LC-MS/MS apparatus to measure the concentration of unchanged compound.

LC-MS/MS Analysis. The LC-MS/MS system consisted of API3200 (Applied Biosystems, Foster City, CA) and LC-20 AD (Shimadzu, Kyoto, Japan) series high-performance liquid chromatography systems fitted with LC-20AD pumps, an SCL-10AVP system controller, an SCL-20AC auto-sampler, and a CTO-20AC column oven (Shimadzu). Analytical conditions are described in Table 1. A flow rate of 0.5 ml/min was used. Ion chromatograms were integrated and quantified using Analyst Software 1.4.1 (Applied Biosystems).

Estimation of Human F_aF_g from In Vivo Pharmacokinetics Data. Human F_aF_g was estimated using eqs. 4 through 6:

$$CL_h = CL_{tot} - CL_r \quad (4)$$

$$F_h = 1 - CL_h/R_b/Q_h \quad (5)$$

$$F_aF_g = F/F_h \quad (6)$$

where CL_h is hepatic clearance, CL_{tot} is plasma-based total clearance, CL_r is renal clearance, Q_h is hepatic blood flow, and F is bioavailability. Because F_aF_g depends on Q_h, three different reference values (17.1, 20.7, and 25.5 ml · min^{-1} · kg^{-1}) were used (Davies and Morris, 1993; Kadono et al., 2010). Pharmacokinetic parameters were derived from the literature. R_b is blood/plasma ratio, which was also obtained from the literature or from in-house data or was assumed to be unity (neutral or basic compound) or 0.55 (acidic compound) if no value was available. For quercetin, because F is not available, this was calculated as in eq. 7:

TABLE 1

Analysis conditions for UGT substrates

Drug	Internal Standard	Mobile Phase	Electrospray Ionization	Transition
Quercetin	Indomethacin	1	Nega	301→151
Raloxifene	Diazepam	1	Posi	474→112
Bazedoxifene	Diazepam	1	Posi	471→126
Diclofenac	Indomethacin	1	Nega	294→250
Tolfenamic acid	Indomethacin	1	Nega	260→216
Tolcapone	Diazepam	1	Posi	274→182
Entacapone	Diazepam	1	Posi	306→233
Telmisartan	Diazepam	1	Posi	515→276
Gemfibrozil	Indomethacin	2	Nega	249→130
Etodolac	Indomethacin	2	Nega	286→242
Indomethacin	Diclofenac	2	Nega	356→312

Phase 1, 0.1% formic acid and 100% acetonitrile; phase 2, 5 mM ammonium formate with 5% acetonitrile and 100% acetonitrile; nega, negative; posi, positive.

$$F = \mathrm{CL_{tot}}/\mathrm{CL_{oral}} \qquad (7)$$

where $\mathrm{CL_{oral}}$ is oral clearance.

Permeability Study Using Artificial Membranes. Drug permeability experiments in parallel artificial membrane permeability assays (PAMPAs) were conducted using PAMPA Evolution from Pion, Inc. (Woburn, MA). PAMPA consisted of a 96-well microtiter plate (Pion, Inc.) and a 96-well filter plate (polyvinylidene difluoride; Millipore Corporation, Billerica, MA), so that each composite was well divided into two chambers, with a donor at the bottom and an acceptor at the top, separated by a 125-μm-thick microfilter disc (0.45-μm pores) coated with a 20% (w/v) dodecane solution of a lecithin mixture (Pion, Inc.). Drugs (10 mM) in dimethyl sulfoxide were prepared in a different 96-well filter plate (polyvinylidene fluoride; Corning Life Science, Lowell, MA) and were added to the donor compartments. The donor solution was adjusted to pH 6.5 (NaOH-treated universal buffer; Pion, Inc.). The plates were sandwiched together and incubated at 25°C for 2 h in a humidity-saturated atmosphere. After incubation, the sandwiched plates were separated, and both the donor and the acceptor compartments were assayed for the amount of material present by comparing their UV spectrums (270–400 nm) with reference standards. Mass balance was used to determine the amount of material remaining in the membrane barrier. The apparent permeability coefficient (P_app) was calculated using PAMPA Evolution software (Pion, Inc.) (eq. 8):

$$P_\mathrm{app} = \frac{V}{A \times C_0} \times \frac{dC}{dt} \qquad (8)$$

where V is the volume of the acceptor chamber, A is the surface area of the cell monolayer, C_0 is the initial substrate concentration, and dC/dt is the change of concentration over time.

Simplified Intestinal Availability Model. F_aF_g was calculated using a theoretical model that combines the permeability and metabolism of epithelial cells as follows (eq. 9):

$$F_aF_g = \frac{\mathrm{CL_{ab}}}{\mathrm{CL_{ab}} + \mathrm{CL_m}} \times \left\{ 1 - \exp\left(-\frac{\mathrm{PS_{inf}}}{Q} \times \frac{\mathrm{CL_{ab}} + \mathrm{CL_m}}{\mathrm{PS_{eff}} + \mathrm{CL_{ab}} + \mathrm{CL_m}} \right) \right\} \qquad (9)$$

where $\mathrm{PS_{inf}}$ is the apparent influx clearance from the lumen to the epithelial cells, $\mathrm{PS_{eff}}$ is the efflux clearance from the cells to the lumen, $\mathrm{CL_{ab}}$ is the absorption clearance from the cells to the blood, $\mathrm{CL_m}$ is the metabolic clearance of the cells, and Q is the luminal flow rate.

Kadono et al. (2010) simplified eq. 9 for highly permeable compounds assuming $\mathrm{PS_{inf}} \gg Q$, $\mathrm{PS_{inf}} \gg \mathrm{PS_{eff}}$ and $\mathrm{CL_{ab}} = $ constant, to give the following (eq. 10):

$$F_aF_g = \frac{1}{1 + \alpha \times \mathrm{CL_m}} \qquad (10)$$

where α is the inverse of $\mathrm{CL_{ab}}$ and is constant. Because it is difficult to estimate α experimentally, in this study $\alpha_\mathrm{int,\ UGT}$ was empirically determined by fitting human F_aF_g and $\mathrm{CLu_{int,\ UGT}}$ in eq. 10 by replacing $\mathrm{CL_m}$ with $\mathrm{CLu_{int,\ UGT}}$.

Data Analysis. GraphPad Prism 5 (GraphPad Software, Inc., La Jolla, CA) was used to fit data for $\mathrm{CLu_{int,\ UGT}}$ and F_aF_g in eq. 10 using the nonlinear least-squares method.

Results

Calculation of Human F_aF_g from In Vivo Human Pharmacokinetic Parameters. Drugs with polar groups show a wide range of structural and physicochemical properties (Supplemental Data 1). More importantly for this study, in humans they all have glucuronide as a metabolite (Table 2). Their pharmacokinetic parameters, including human F_aF_g, are summarized in Table 3. Because F_aF_g values were sensitive to hepatic blood flow, three different human hepatic blood flows were used to determine human F_aF_g values, although this had a minimal effect on their rank order.

In Vitro Intrinsic Clearance. In vitro intrinsic clearance values are summarized in Table 4. In vitro intrinsic clearance by human intes-

TABLE 2

Metabolic pathway

Drug	Metabolic Pathway	References
Quercetin	Glucuronidation	Graefe et al., 2001
Raloxifene	Glucuronidation	Jones, 1997
Bazedoxifene	Glucuronidation, oxidation	Chandrasekaran et al., 2009
Diclofenac	Glucuronidation, oxidation	Stierlin et al., 1979
		Stierlin and Faigle, 1979
Tolfenamic acid	Glucuronidation	Pentikäinen et al., 1984
Tolcapone	Glucuronidation, oxidation, methylation	Jorga et al., 1999
Entacapone	Glucuronidation	Wikberg et al., 1993
Telmisartan	Glucuronidation	Stangier et al., 2000
Gemfibrozil	Glucuronidation, oxidation	Okerholm et al., 1976
Etodolac	Glucuronidation, oxidation	Ferdinandi et al., 1986
Indomethacin	Oxidation, glucuronidation	Duggan et al., 1972

tinal UGT ($\mathrm{CL_{int,\ UGT}}$) ranged from 4.2 (indomethacin) to 4620 $\mu\mathrm{l} \cdot \mathrm{min^{-1}} \cdot \mathrm{mg^{-1}}$ (quercetin). Corrected $\mathrm{CL_{int,\ UGT}}$ ($\mathrm{CLu_{int,\ UGT}}$; eq. 3) ranged from 5.2 (indomethacin) to 5133 (quercetin) $\mu\mathrm{l} \cdot \mathrm{min^{-1}} \cdot \mathrm{mg^{-1}}$. No apparent unchanged drug decrease was detected in human intestinal cytochrome P450 (P450) metabolism for all drugs except raloxifene and bazedoxifene. For these two drugs the in vitro intrinsic clearance by human intestinal P450s ($\mathrm{CL_{int,\ P450}}$) were 8.9 and 4.7 $\mu\mathrm{l} \cdot \mathrm{min^{-1}} \cdot \mathrm{mg^{-1}}$, respectively. For all substrates, $\mathrm{CL_{int,\ UGT}}$ was much higher than $\mathrm{CL_{int,\ P450}}$.

Permeability. The permeability of each substrate was examined using an artificial membrane. P_app values are summarized in Table 5. A high F_a can be expected when the P_app value is greater than 1.0×10^{-6} cm/s (Kadono et al., 2010), which was seen in all 11 substrates except for quercetin and gemfibrozil.

Relationship between $\mathrm{CLu_{int,\ UGT}}$ and F_aF_g. Figure 1 shows an inverse relationship between $\mathrm{CLu_{int,\ UGT}}$ and F_aF_g for all three hepatic blood flows. To investigate the validity of the model, goodness-of-fit values of the SIA model and linear relationship were compared. The r^2 of the SIA model (0.92) was found to be higher than that of the linear model (0.58), indicating that the SIA model is more suitable. Human $\alpha_\mathrm{int,\ UGT}$ for each hepatic blood flow was determined by the SIA model and is shown in Table 6.

Identification of UGT Substrates Contributing to Glucuronidation. Twelve commercially available recombinant human UGTs expressed in insect cells were used to identify those UGT isoforms that contribute to glucuronidation (Fig. 2). Certain isoforms resulted in significantly lower remaining ratios for specific drugs. For example, the remaining ratio for quercetin, which had the lowest F_aF_g value of all substrates examined, was insignificant for the isoforms UGT1A3 and UGT1A1. For raloxifene and bazedoxifene, which also had relatively low F_aF_g values, the remaining ratios for UGT1A8 and UGT1A10 were much lower than those for other isoforms. Tolfenamic acid, whose UGT isoforms have not been reported, was significantly metabolized by UGT1A1, UGT1A7, UGT1A9, UGT2B7, and UGT2B15, although its remaining ratio was significantly lower in response to UGT1A9 and UGT2B7.

Comparison of Empirical Scaling Factors. Differences between intestinal P450s and UGTs in humans or differences between rat and human $\alpha_\mathrm{int,\ UGT}$ in the SIA model fitting curves were compared. The empirical scaling factor human $\alpha_\mathrm{met,\ P450} = 0.64$ was determined by the relationship between $\mathrm{CL_{met,\ P450}}$ and human F_aF_g at a hepatic blood flow of 20.7 ml · min^{-1} · kg^{-1}, which is cited from a previous study (Kadono et al., 2010). $\mathrm{CL_{met,\ P450}}$ is $\mathrm{CL_{int,\ P450}}$ corrected by the $\mathrm{CL_{int,\ P450}}$ of midazolam to normalize the lot difference of intestinal microsomes, indicating that $\alpha_\mathrm{met,\ P450}$ is a constant value among pooled HIM. The $\mathrm{CL_{int,\ P450}}$ of midazolam was determined by intestinal microsomes ($\mathrm{CL_{int,\ P450}} = 123$ $\mu\mathrm{l} \cdot \mathrm{min^{-1}} \cdot \mathrm{mg^{-1}}$) in this study.

TABLE 3

Pharmacokinetic parameters for 11 UGT substrates

Drug	CL_{tot}	R_b	CL_r	F	F_aF_g			Reference
					17.1	20.7	25.5	
	$ml \cdot min^{-1} \cdot kg^{-1}$		$ml \cdot min^{-1} \cdot kg^{-1}$		Q_h ($ml \cdot min^{-1} \cdot kg^{-1}$)			
Quercetin	11	1.0	0	0.001[a]	0.004	0.003	0.002	Cubitt et al., 2009
Raloxifene	14.7[b]	1.0	0	0.02	0.143	0.069	0.047	Thummel et al., 2005
Bazedoxifene	6.7[c]	0.55	0	0.06	0.145	0.117	0.101	Patat et al., 2003; Chandrasekaran et al., 2009
								Chandrasekaran et al., 2003
Diclofenac	3.5	0.63	0	0.54	0.800	0.738	0.690	Willis et al., 1979
								Obach et al., 2008
Tolfenamic acid	2.2	0.66	0	0.60	0.745	0.715	0.690	Pentikäinen et al., 1981
Tolcapone	1.9	0.61	0	0.60	0.734	0.706	0.683	Jorga et al., 1998
								Obach et al., 2008
Entacapone	12	0.59	0	0.25	1.00[e]	1.00[f]	1.00[f]	Heikkinen et al., 2001
								Obach et al., 2008
Telmisartan	8.4	0.67	0	0.43	1.00[e,f]	1.00[f]	0.846[f]	Obach et al., 2008
								Stangier et al., 2000
Gemfibrozil	1.7	0.58	0	0.98	1.00[f]	1.00[f]	1.00[f]	Thummel et al., 2005
Etodolac	0.66[d]	0.55	0	0.80	0.859	0.848	0.839	
Indomethacin	1.4	0.55[g]	0.21	1.0	1.00[f]	1.00[f]	1.00[f]	Thummel et al., 2005

[a] Calculated from CL_{tot} (11 $ml \cdot min^{-1} \cdot kg^{-1}$) and oral clearance (8333 $ml \cdot min^{-1} \cdot kg^{-1}$) (Cubitt et al., 2009).
[b] Calculated from oral clearance data (735 $ml \cdot min^{-1} \cdot kg^{-1}$) and reported bioavailability of 2% (Thummel et al., 2005).
[c] Calculated from oral clearance data (86.7 $ml \cdot min^{-1} \cdot kg^{-1}$) and reported bioavailability of 6.2% (Patat et al., 2003; Chandrasekaran et al., 2009).
[d] Calculated from oral clearance data (0.82 $ml \cdot min^{-1} \cdot kg^{-1}$) and reported bioavailability of 80%. Etodolac (Lodine) U.S. Food and Drug Administration drug approval package (http://www.accessdata.fda.gov/drugsatfda_docs/label/2006/018922s022,020584s009lbl.pdf).
[e] Calculated F_aF_g was < 0, because $CL_{tot}/R_b/Q_h$ was > 1. Therefore, CL_{tot}/R_b was assumed to 90% of Q_h.
[f] When calculated F_aF_g was > 1, it was treated as 1.0.
[g] Assumed to be 0.55 because indomethacin and etodolac are acidic drugs (Cubitt et al., 2011).

Therefore, the empirical scaling factor human $\alpha_{int, P450}$ was calculated by dividing $\alpha_{met, P450}$ by $CL_{int, P450}$ of midazolam, resulting in $\alpha_{int, P450} = 5.2 \times 10^{-3}$ at a hepatic blood flow of 20.7 $ml \cdot min^{-1} \cdot kg^{-1}$. The fitting curves for human $\alpha_{int, UGT}$ and human $\alpha_{int, P450}$ were almost identical (Fig. 3A), indicating that the SIA model could indeed be applicable with UGT and P450 substrates using the same α value. On the other hand, rats showed different results. The empirical scaling factor rat $\alpha_{int, UGT} = 0.0021$ was obtained from the relationship between rat $CL_{int, UGT}$ and rat F_aF_g described by Furukawa et al. (2012). As seen in Fig. 3B, rat $\alpha_{int, UGT}$ was less than the human $\alpha_{int, UGT}$, resulting in distinct fitting curves (Fig. 3 B).

Discussion

Increasing awareness of the importance of intestinal glucuronidation has led to the need to predict this pathway's first-pass effect on drugs during the discovery stage. However, a reliable method for quantitatively predicting this effect is still lacking. The aim of this study was to consider a method for predicting the effect of intestinal glucuronidation on human intestinal availability.

The SIA model showed that $CLu_{int, UGT}$ and F_aF_g have an inverse relationship (Fig. 1). This indicates that for highly permeable UGT substrates as well as CYP3A4 substrates, F_aF_g could be predicted by combining in vitro data and the SIA model. However, because of limitations in the SIA model, it is necessary that the substrates tested have high permeability. Except for quercetin and gemfibrozil, all substrates tested had P_{app} values $> 1.0 \times 10^{-6}$ cm/s, indicating high absorption in human intestine (Kadono et al., 2010). Consequently, human F_a values are expected to be high. Despite its low P_{app} value, quercetin too is expected to have a high human F_a (Walgren et al., 1998), because it has been reported that 65 to 81% of quercetin is

TABLE 4

In vitro intrinsic clearance by UGTs in HIM ($CL_{int, UGT}$), unbound $CL_{int, UGT}$ ($CLu_{int, UGT}$); in vitro intrinsic clearance by P450s in HIM ($CL_{int, CYP}$), unbound $CL_{int, P450}$ ($CLu_{int, P450}$)

Drug	UGT			P450		
	$f_{u, mic}$	$CL_{int, UGT}$	$CLu_{int, UGT}$	$f_{u, mic}$	$CL_{int, P450}$	$CLu_{int, P450}$
		$\mu l \cdot min^{-1} \cdot mg^{-1}$	$\mu l \cdot min^{-1} \cdot mg^{-1}$	mg/ml	$\mu l \cdot min^{-1} \cdot mg^{-1}$	$\mu l \cdot min^{-1} \cdot mg^{-1}$
Quercetin	0.90[a]	4620 ± 800[b]	5133	NT	N.D.	N.D.
Raloxifene	0.98 ± 0.11[b]	2180 ± 60[b]	2224	0.43 ± 0.06[d]	8.90 ± 0.16[d]	20.7
Bazedoxifene	0.38 ± 0.05[c]	166 ± 2[c]	437	0.16 ± 0.01[d]	4.70 ± 0.36[d]	29.4
Diclofenac	0.94 ± 0.05[c]	59.0 ± 4.4[c]	62.7	N.T.	N.D.	N.D.
Tolfenamic acid	0.88 ± 0.10[c]	155 ± 5[c]	176	N.T.	N.D.	N.D.
Tolcapone	0.39 ± 2[c]	40.0 ± 0.5[c]	103	N.T.	N.D.	N.D.
Entacapone	1.00 ± 0.2[c]	27.0 ± 3.8[c]	27.0	N.T.	N.D.	N.D.
Telmisartan	0.92 ± 0.05[c]	20.0 ± 2.0[c]	21.7	N.T.	N.D.	N.D.
Gemfibrozil	0.97 ± 0.04[c]	17.0 ± 2.1[c]	17.5	N.T.	N.D.	N.D.
Etodolac	1.1 ± 0.1[d]	6.20 ± 0.86[d]	5.7	N.T.	N.D.	N.D.
Indomethacin	0.80 ± 0.06[d]	4.20 ± 0.67[d]	5.2	N.T.	N.D.	N.D.

N.T., not tested; N.D., no depletion.
[a] The $f_{u, mic}$ value of quercetin is cited from (Cubitt et al., 2009) because of degradation during equilibrium dialysis. Data are given as mean $\pm$ S.D.
[b] Microsomal protein concentration was 0.02 mg/ml.
[c] Microsomal protein concentration was 0.2 mg/ml.
[d] Microsomal protein concentration was 0.4 mg/ml.

TABLE 5

Permeability in artificial membrane

Drug	$P_{app} \times 10^{-6}$ cm/s
Quercetin	<1.5
Raloxifene	3.0
Bazedoxifene	20
Diclofenac	22
Tolfenamic acid	14
Tolcapone	18
Entacapone	4.1
Telmisartan	>30
Gemfibrozil	<0.1
Etodolac	23
Indomethacin	22

TABLE 6

Empirical scaling factor (human $\alpha_{int, UGT}$) of the SIA model obtained from 11 UGT substrates under three hepatic blood flow conditions (Q_h)

Substrate	Q_h		
	17.1	20.7	25.5
	$ml \cdot min^{-1} \cdot kg^{-1}$		
Human $\alpha_{int, UGT}$	3.8×10^{-3}	4.4×10^{-3}	5.2×10^{-3}

absorbed after oral administration in humans (Graefe et al., 2001). Gemfibrozil is also expected to have a high F_a value, because its bioavailability is approximately 100% (Thummel et al., 2005).

The inverse relationship is strengthened by the fact that all substrates tested are expected to be metabolized mainly by UGTs in the human intestine, because all but tolcapone are metabolized by P450s and UGTs (Table 2). Although an oxidized metabolite was detected in human plasma after the oral administration of diclofenac, gemfibrozil, etodolac, and indomethacin, there was no decrease in the unchanged compound in HIM involving NADPH, indicating that intestinal P450 metabolism does not contribute to the intestinal metabolism. Only raloxifene and bazedoxifene had their $CL_{int, P450}$ values determined, with both being significantly less than their respective $CL_{int, UGT}$ values, indicating that glucuronidation contributes to human intestinal metabolism. Although one main metabolite in humans after the oral administration of tolcapone was glucuronide, a methylated metabolite was also detected (Jorga et al., 1999). This methylation is mediated through catechol-*O*-methyltransferase enzyme (COMT). However, because COMT activity is low (Ellingson et al., 1999), and because the main metabolite was glucuronide, it is unlikely that intestinal COMT affects the $F_a F_g$ of tolcapone. These results are consistent with the inverse relationship between $CLu_{int, UGT}$ and $F_a F_g$.

Given that oral area under the concentration-time curve (AUC) values of our selected drugs increase in almost direct proportion to oral dose (Supplemental Data 2), we conducted in vitro metabolism experiments at a relatively low concentration of 0.1 μM, which is

believed to be lower than general K_m values of UGTs (Williams et al., 2004). However, the predicted concentrations in human intestine (Supplemental Data 3) were much higher than 0.1 μM, indicating that intestinal glucuronidation should be saturated, which contradicts the linearity of oral AUC increases. For example, a previous study found that K_m values of bazedoxifene for intestinal microsomes—5.1 (bazedoxifene-4′-glucuronide) and 5.1 μM (bazedoxifene-6′-glucuronide) (Shen et al., 2010)—were lower than the predicted intestinal concentration (25–170 μM) at oral doses ranging from 3 to 20 mg (Supplemental Data 3); however, oral AUC values were reported to increase in proportion to oral doses from 5 to 120 mg (Supplemental Data 2). This contradiction may be explained by autoactivation and gut volume. Autoactivation has been reported for UGT substrates (Wong et al., 2007), indicating that intestinal glucuronidation may not be saturated at concentrations close to K_m values. The predicted intestinal concentration is traditionally calculated by dividing molar dose by 250 ml, the estimated volume of a glass of water. However, given that 250 ml has been reported to be smaller than the calculated intestinal fluid volume, intestinal drug-drug interaction predictions may be overestimated when 250 ml is used (Tachibana et al., 2009). Therefore, further investigation will be required to clarify the kinetics of UGTs and the concentration in human intestine.

To clarify the UGT isoforms that contribute to the glucuronidation of each substrate, UGT isoform phenotyping was conducted using hrUGTs. Depending on the substrate, specific UGT isoforms significantly decreased the remaining ratio. For example, for raloxifene, the glucuronidation rates of UGT1A8, UGT1A9, and UGT1A10 are reported to be higher than those of other isoforms (Kemp et al., 2002), which is consistent with our remaining ratio results. Similar consistencies were found with bazedoxifene for UGT1A1, UGT1A8, and UGT1A10 (Shen et al., 2010), diclofenac and gemfibrozil for
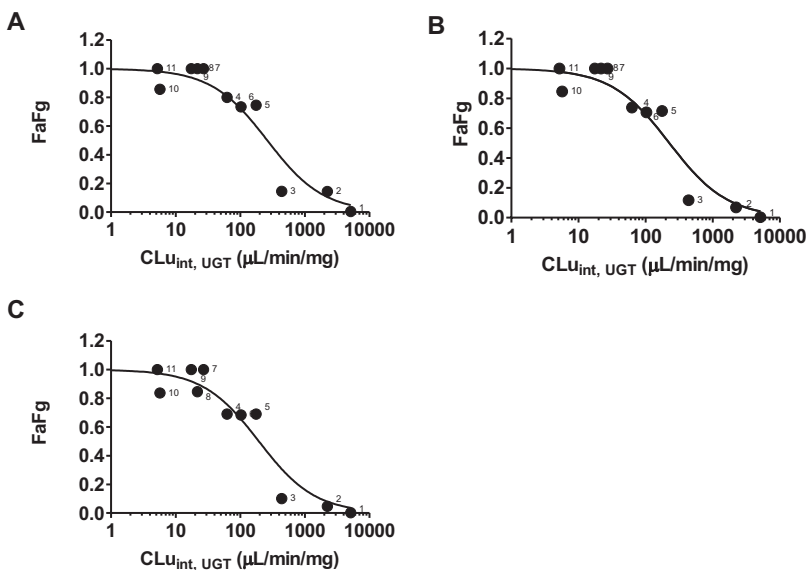

FIG. 1. Relationship between $CLu_{int, UGT}$ and $F_a F_g$ for 11 model substrates under three hepatic blood flow conditions: 17.7 (A), 20.7 (B), and 25.5 ml · min^{-1} · kg^{-1} (C). Solid lines were obtained by fitting with the nonlinear least-squares method. When an observed $F_a F_g$ was more than 1, it was treated as 1.0. 1, quercetin; 2, raloxifene; 3, bazedoxifene; 4, diclofenac; 5, tolfenamic acid; 6, tolcapone; 7, entacapone; 8, telmisartan; 9, gemfibrozil; 10, etodolac; and 11, indomethacin.
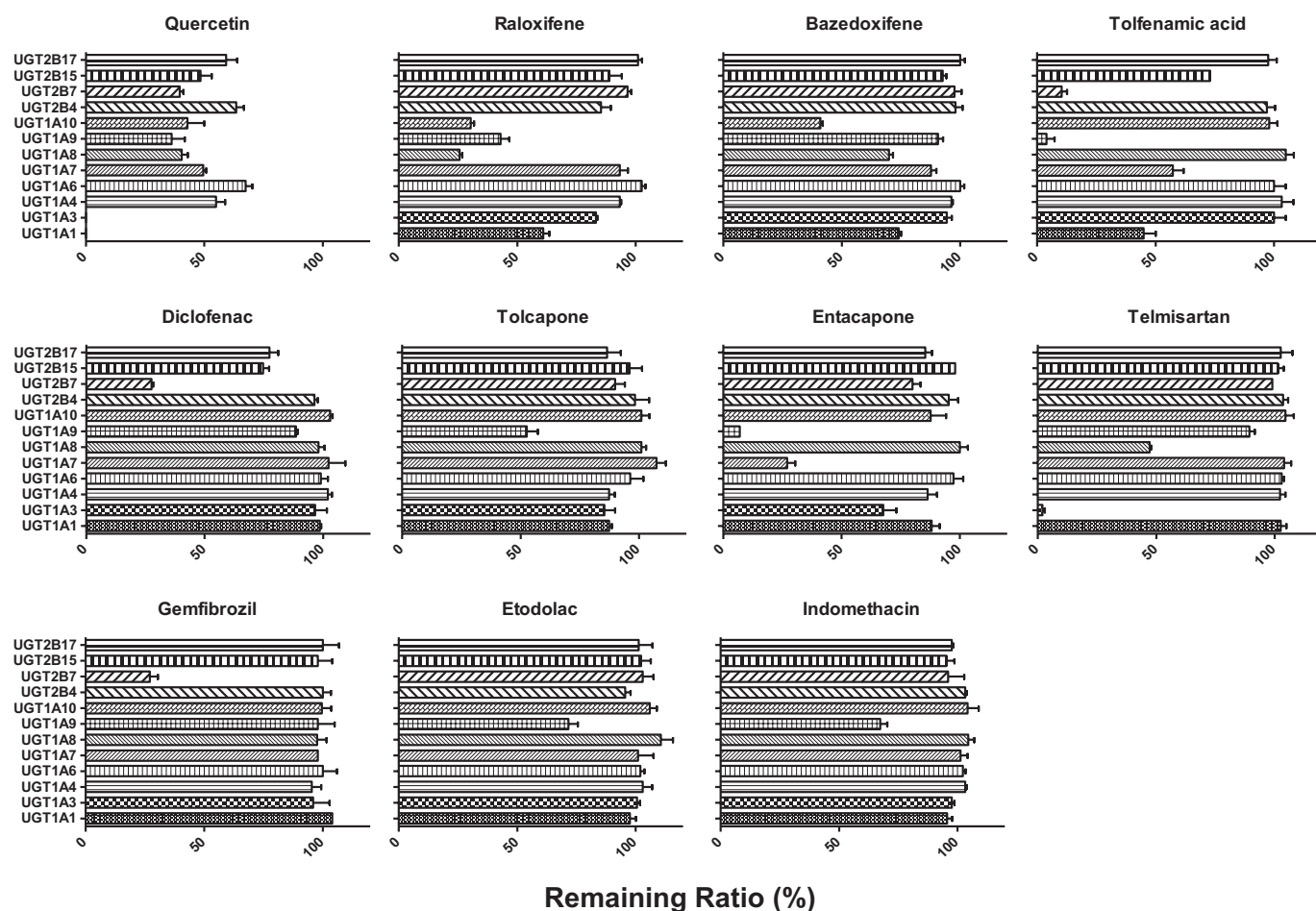
FIG. 2. Rate of decrease of unchanged compound during incubation experiments with recombinant human UGT isoforms. Each column represents the remaining ratio after 30 min of incubation. Error bars are S.D. of the mean for triplicate samples.

UGT2B7, and tolcapone, etodolac, and indomethacin for UGT1A9. Overall, these results indicate that the substrates were metabolized by various UGT isoforms, and that the SIA model was applicable independent of the isoform.

The empirical scaling factor, α, which was obtained by fitting the relationship between human F_aF_g and intestinal intrinsic clearance, may be a hybrid of the human mucosal blood flow and a scale-up number of the ratio of UGT activity per intestinal microsome to UGT activity per body weight. The scale-up number describes glucuronidation activity per microsomal activity to glucuronidation activity per body weight and is needed to meet the unity of Q_{ent} (ml · min^{-1} · kg^{-1}). This is for several reasons. First, the Q_{gut} model (Yang et al., 2007) predicts human F_g from in vitro metabolic clearance and membrane permeability as follows (eqs. 11 and 12):

$$F_g = Q_{gut}/(Q_{gut} + f_{ugut} \times CL_{int,in\ vitro}) \qquad (11)$$

$$Q_{gut} = CL_{perm} \times Q_{ent}/(Q_{ent} + CL_{perm}) \qquad (12)$$

where Q_{ent} is mucosal blood flow, f_{ugut} is the fraction of unbound drug in enterocytes, and CL_{perm} is permeability clearance, which is defined as the product of intestinal surface area and apparent or effective permeability. Yang et al. (2007) assumed $f_{ugut} = 1$ when applying the Q_{gut} model. Furthermore, for highly permeable substrates, it can be assumed that $CL_{perm} \gg Q_{ent}$, leading to the following (eq. 13):

$$F_g = 1/(1 + CL_{int,\ in\ vitro}/Q_{ent}) \qquad (13)$$

By combining eqs. 9 and 13, one can show the empirical scaling factor equals the reciprocal of enterocytic blood flow corrected by the scale-up factor (that is, α = scale-up number/Q_{ent}). Second, human $\alpha_{int,\ UGT}$ values resembled human $\alpha_{int,\ P450}$ values independently of the metabolic enzyme (Fig. 3A). This result indicates that α represents a physiological parameter such as blood flow. Third, the rank order that human $\alpha_{int,\ UGT}$ is greater than rat $\alpha_{int,\ UGT}$ is consistent with the rank order of human scale-up number/Q_{ent} being higher than rat scale-up number/Q_{ent}. For example, the values of mucosal blood flow are 4.6 in humans (Soars et al., 2002) and 14.4 ml · min^{-1} · kg^{-1} in rats, the latter being obtained by correcting rat Q_{ent} with a rat body weight of 0.25 kg (Davies and Morris, 1993; Yang et al., 2007). The scale-up number has been reported to be 90 in humans (Soars et al., 2002) and 34 mg/kg b.wt. in rats (Yoon et al., 2011). Therefore, the scale-up number/Q_{ent} in humans is 0.020 and in rats is 0.0024 min · kg/μl. The rank order of $\alpha_{int,\ UGT}$ between rats and humans is consistent with that of the scale-up number/Q_{ent}, indicating that the empirical scaling factor α is in fact equivalent to the scale-up number/Q_{ent} value. However, to validate this hypothesis, far more intestinal microsomes need to be investigated.

In summary, for highly permeable UGT substrates, $CL_{int,\ UGT}$ and F_aF_g showed an inverse relationship, indicating F_aF_g can be predicted by combining in vitro glucuronidation measurements and the SIA model. These insights indicate that in vitro glucuronidation studies and the SIA model may be able to predict the impact of intestinal glucuronidation on the first-pass effect in humans.
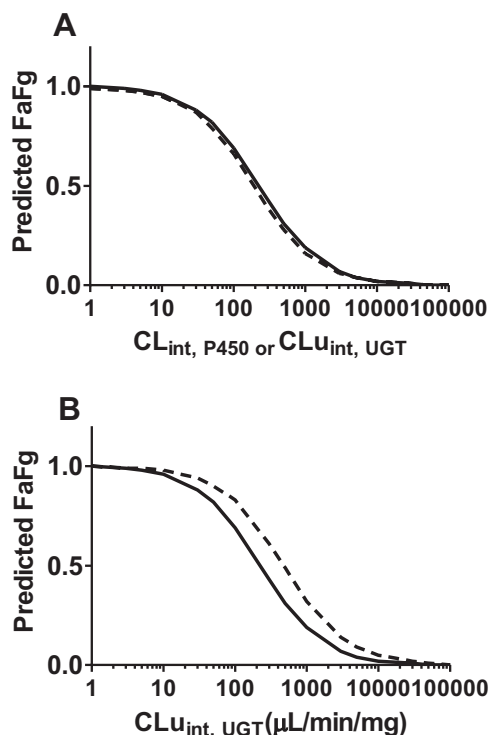
FIG. 3. Comparison of fitting curves between predicted F_aF_g and in vitro glucuronidation clearance. A, the solid line represents the fitting curve obtained from the relationship between $CLu_{int, UGT}$ and human F_aF_g; the dotted line represents that obtained from the relationship between $CL_{int, P450}$ and human F_aF_g. B, the solid line represents the fitting curve obtained from the relationship between $CLu_{int, UGT}$ and human F_{aFg}; the dotted line represents that obtained from the relationship between $CLu_{int, UGT}$ and F_aF_g in rats.

References

Chandrasekaran A, Ermer J, McKeand W, Lee H, DeMaio W, Kotake A, Sullivan P, Orczyk G, and Scatina J (2003) Bazedoxifene acetate metabolic disposition in healthy, postmenopausal women (Abstract). *Clin Pharmacol Ther* 73:47.

Chandrasekaran A, McKeand WE, Sullivan P, DeMaio W, Stoltz R, and Scatina J (2009) Metabolic disposition of [14C]bazedoxifene in healthy postmenopausal women. *Drug Metab Dispos* 37:1219–1225.

Cubitt HE, Houston JB, and Galetin A (2009) Relative importance of intestinal and hepatic glucuronidation-impact on the prediction of drug clearance. *Pharm Res* 26:1073–1083.

Cubitt HE, Houston JB, and Galetin A (2011) Prediction of human drug clearance by multiple metabolic pathways: integration of hepatic and intestinal microsomal and cytosolic data. *Drug Metab Dispos* 39:864–873.

Davies B and Morris T (1993) Physiological parameters in laboratory animals and humans. *Pharm Res* 10:1093–1095.

Duggan DE, Hogans AF, Kwan KC, and McMahon FG (1972) The metabolism of indomethacin in man. *J Pharmacol Exp Ther* 181:563–575.

Ellingson T, Duddempudi S, Greenberg BD, Hooper D, and Eisenhofer G (1999) Determination of differential activities of soluble and membrane-bound catechol-O-methyltransferase in tissues and erythrocytes. *J Chromatogr B Biomed Sci Appl* 729:347–353.

Ferdinandi ES, Sehgal SN, Demerson CA, Dubuc J, Zilber J, Dvornik D, and Cayen MN (1986) Disposition and biotransformation of 14C-etodolac in man. *Xenobiotica* 16:153–166.

Furukawa T, Nakamori F, Tetsuka K, Naritomi Y, Moriguchi H, Yamano K, Terashita S, and Teramura T (2012) Quantitative prediction of intestinal glucuronidation of drugs in rats using in vitro metabolic clearance data. *Drug Metab Pharmacokinet* 27:171–180.

Graefe EU, Wittig J, Mueller S, Riethling AK, Uehleke B, Drewelow B, Pforte H, Jacobasch G, Derendorf H, and Veit M (2001) Pharmacokinetics and bioavailability of quercetin glycosides in humans. *J Clin Pharmacol* 41:492–499.

Heikkinen H, Saraheimo M, Antila S, Ottoila P, and Pentikäinen PJ (2001) Pharmacokinetics of entacapone, a peripherally acting catechol-O-methyltransferase inhibitor, in man. A study using a stable isotope techique. *Eur J Clin Pharmacol* 56:821–826.

Jones C (1997) Clinical pharmacology & biopharmaceutical review for EVISTA[TM]. Submitted to FDA Dec 9; NDA 20-815.

Jorga K, Fotteler B, Heizmann P, and Gasser R (1999) Metabolism and excretion of tolcapone, a novel inhibitor of catechol-O-methyltransferase. *Br J Clin Pharmacol* 48:513–520.

Jorga KM, Fotteler B, Heizmann P, and Zürcher G (1998) Pharmacokinetics and pharmacodynamics after oral and intravenous administration of tolcapone, a novel adjunct to Parkinson's disease therapy. *Eur J Clin Pharmacol* 54:443–447.

Kadono K, Akabane T, Tabata K, Gato K, Terashita S, and Teramura T (2010) Quantitative prediction of intestinal metabolism in humans from a simplified intestinal availability model and empirical scaling factor. *Drug Metab Dispos* 38:1230–1237.

Kemp DC, Fan PW, and Stevens JC (2002) Characterization of raloxifene glucuronidation in vitro: contribution of intestinal metabolism to presystemic clearance. *Drug Metab Dispos* 30:694–700.

Mizuma T (2009) Intestinal glucuronidation metabolism may have a greater impact on oral bioavailability than hepatic glucuronidation metabolism in humans: a study with raloxifene, substrate for UGT1A1, 1A8, 1A9, and 1A10. *Int J Pharm* 378:140–141.

Nakamori F, Naritomi Y, Furutani M, Takamura F, Miura H, Murai H, Terashita S, and Teramura T (2011) Correlation of intrinsic in vitro and in vivo clearance for drugs metabolized by hepatic UDP-glucuronosyltransferases in rats. *Drug Metab Pharmacokinet* 26:465–473.

Obach RS, Lombardo F, and Waters NJ (2008) Trend analysis of a database of intravenous pharmacokinetic parameters in humans for 670 drug compounds. *Drug Metab Dispos* 36:1385–1405.

Ohno S and Nakajin S (2009) Determination of mRNA expression of human UDP-glucuronosyltransferases and application for localization in various human tissues by real-time reverse transcriptase-polymerase chain reaction. *Drug Metab Dispos* 37:32–40.

Okerholm RA, Keeley FJ, Peterson FE, and Glazko AJ (1976) The metabolism of gemfibrozil. *Proc R Soc Med* 69 (Suppl 2):11–14.

Patat A, McKeand W, Baird-Bellaire S, Ermer J, and LeCoz F (2003) Absolute bioavailability of bazedoxifene acetate in healthy postmenopausal women (Abstract). *Clin Pharmacol Ther* 73:43.

Pentikäinen PJ, Neuvonen PJ, and Backman C (1981) Human pharmacokinetics of tolfenamic acid, a new anti-inflammatory agent. *Eur J Clin Pharmacol* 19:359–365.

Pentikäinen PJ, Tokola O, Alhava E, and Penttilä A (1984) Pharmacokinetics of tolfenamic acid: disposition in bile, blood and urine after intravenous administration to man. *Eur J Clin Pharmacol* 27:349–354.

Shen L, Ahmad S, Park S, DeMaio W, Oganesian A, Hultin T, Scatina J, Bungay P, and Chandrasekaran A (2010) In vitro metabolism, permeability, and efflux of bazedoxifene in humans. *Drug Metab Dispos* 38:1471–1479.

Soars MG, Burchell B, and Riley RJ (2002) In vitro analysis of human drug glucuronidation and prediction of in vivo metabolic clearance. *J Pharmacol Exp Ther* 301:382–390.

Stangier J, Schmid J, Türck D, Switek H, Verhagen A, Peeters PA, van Marle SP, Tamminga WJ, Sollie FA, and Jonkman JH (2000) Absorption, metabolism, and excretion of intravenously and orally administered [14C]telmisartan in healthy volunteers. *J Clin Pharmacol* 40:1312–1322.

Stierlin H and Faigle JW (1979) Biotransformation of diclofenac sodium (Voltaren) in animals and in man. II. Quantitative determination of the unchanged drug and principal phenolic metabolites, in urine and bile. *Xenobiotica* 9:611–621.

Stierlin H, Faigle JW, Sallmann A, Küng W, Richter WJ, Kriemler HP, Alt KO, and Winkler T (1979) Biotransformation of diclofenac sodium (Voltaren) in animals and in man. I. Isolation and identification of principal metabolites. *Xenobiotica* 9:601–610.

Tachibana T, Kato M, Watanabe T, Mitsui T, and Sugiyama Y (2009) Method for predicting the risk of drug-drug interactions involving inhibition of intestinal CYP3A4 and P-glycoprotein. *Xenobiotica* 39:430–443.

Thummel KE, Shen DP, Isoherran N, and Smith HE (2005) Design and optimization of dosage regimes: pharmacokinetic data, in *Goodman & Gilman's the Pharmacological Basis of Therapeutics* (Brunton LL, Chabner BA, and Knollmann BC eds) 12th ed, pp 1787–1888, McGraw-Hill, New York.

Walgren RA, Walle UK, and Walle T (1998) Transport of quercetin and its glucosides across human intestinal epithelial Caco-2 cells. *Biochem Pharmacol* 55:1721–1727.

Wikberg T, Vuorela A, Ottoila P, and Taskinen J (1993) Identification of major metabolites of the catechol-O-methyltransferase inhibitor entacapone in rats and humans. *Drug Metab Dispos* 21:81–92.

Williams JA, Hyland R, Jones BC, Smith DA, Hurst S, Goosen TC, Peterkin V, Koup JR, and Ball SE (2004) Drug-drug interactions for UDP-glucuronosyltransferase substrates: a pharmacokinetic explanation for typically observed low exposure (AUCi/AUC) ratios. *Drug Metab Dispos* 32:1201–1208.

Willis JV, Kendall MJ, Flinn RM, Thornhill DP, and Welling PG (1979) The pharmacokinetics of diclofenac sodium following intravenous and oral administration. *Eur J Clin Pharmacol* 16:405–410.

Wong H, Tong V, Riggs KW, Rurak DW, Abbott FS, and Kumar S (2007) Kinetics of valproic acid glucuronidation: evidence for in vivo autoactivation. *Drug Metab Dispos* 35:1380–1386.

Yang J, Jamei M, Yeo KR, Tucker GT, and Rostami-Hodjegan A (2007) Prediction of intestinal first-pass drug metabolism. *Curr Drug Metab* 8:676–684.

Yoon IS, Choi MK, Kim JS, Shim CK, Chung SJ, and Kim DD (2011) Pharmacokinetics and first-pass elimination of metoprolol in rats: contribution of intestinal first-pass extraction to low bioavailability of metoprolol. *Xenobiotica* 41:243–251.

Address correspondence to: Fumihiro Nakamori, Astellas Pharma, Inc., Analysis and Pharmacokinetics Research Laboratories, 21 Miyukigaoka, Tsukuba, Ibaraki, 305-8585, Japan. E-mail: fumihiro.nakamori@astellas.com